Energy, Mines and Resources Canada

Énergie, Mines et Ressources Canada

CANMET

Canada Centre for Mineral and Energy Technology

Centre canadien de la technologie des minéraux et de l'énergie

Metals Technology Laboratories

Laboratoires de la technologie des métaux

Canada

METALS TECHNOLOGY LABORATORIES

EVALUATION OF ALUMINA/ZN-27AL METAL MATRIX COMPOSITES

S. DIONNE, J. LO, L. DIGNARD-BAILEY AND M. SAHOO

MTL 89-81(TR)

This document is an unedited interim report prepared primarily for discussion and internal reporting purposes. It does not represent a final expression of the opinion of the Canada Centre for Mineral and Energy Technology (CANMET)

Ce document est un rapport provisoire non-révisé et rédigé principalement pour fin de discussion et de documentation interne. Il ne représente nullement l'expression définitive de l'opinion du Centre canadien de la technologie des minéraux et de l'énergie (CANMET)

MICROMEDIA

41 pp

CANMET

90-07114/

METALS TECHNOLOGY LABORATORIES
REPORT MTL89-81(TR)

EVALUATION OF ALUMINA/ZN-27AL METAL MATRIX COMPOSITES

by

S. Dionne, J. Lo, L. Dignard-Bailey and M. Sahoo

SUMMARY

Over recent years, commercial Zn-Al foundry alloys such as ZA 27 have found increasing use in many applications and have effectively competed against copper, aluminum and iron-based foundry alloys. However, Zn-Al alloys suffer from poor elevated temperature properties which restrict their performance for some applications. The purpose of this investigation was therefore to examine the effects of alumina fibre reinforcement on the elevated temperature properties of a Zn-Al foundry alloy (Zn-27%Al-2%Cu-0.01%Mg). Billets of unreinforced Zn-Al matrix alloy, 10 vol% Al_2O_3/Zn-27Al and 20 vol% Al_2O_3/Zn-27Al were fabricated by squeeze casting. The chemical composition, reinforcement distribution and microstructure of these materials were characterized. Tensile and impact properties were evaluated at 25°C, 100°C and 150°C as well as compression and fatigue properties at 25°C and 100°C. Wear and creep tests also were performed on the unreinforced alloy and composites. Fractographic examinations were carried out to determine the operative fracture mechanisms.

It was found that although fibre reinforcement did result in some improvement of tensile and compression properties at elevated temperatures, the composites had poor toughness and ductility. The presence of a brittle SiO_2 layer at the fibre/matrix interfaces resulted in extensive fibre/matrix decohesion under tensile loading, severely impairing the performance of the reinforced materials. Some improvement in wear resistance was noted for the composite materials but fibre reinforcement did not yield any notable improvement in fatigue resistance.

LABORATOIRES DE LA TECHNOLOGIE DES MÉTAUX
RAPPORT MTL 89-81(TR)

ÉVALUATION DES COMPOSITES À MATRICE MÉTALLIQUE ALUMINE/ZN-27 AL

par

S. Dionne, J. Lo, L. Dignard-Bailey et M. Sahoo

SOMMAIRE

Depuis quelques années, les alliages de fonderie Zn-Al commerciaux comme le ZA-27 sont de plus en plus utilisés dans de nombreuses applications et mènent une vive concurrence aux alliages de fonderie à base de cuivre, d'aluminium et de fer. Toutefois, aux températures élevées les alliages Zn-Al ont des propriétés médiocres qui limitent leur rendement dans certaines applications. Le but de cette étude était donc d'examiner les effets de l'addition de fibres de renforcement en alumine sur les propriétés à haute température d'un alliage de fonderie Zn-Al (Zn-27%Al-2%Cu-0,1%Mg). Des billettes à matrice Zn-Al non renforcé et d'alliage Zn-Al, contenant 10% et 20% en volume de Al_2O_3 ont été fabriquées par coulée sous pression. La composition chimique, la distribution des fibres de renforcement et la microstructure de ces matériaux ont été caractérisées. Les propriétés en traction et en impact ont été évaluées à 25, 100 et 150°C, ainsi que les propriétés en compression et en fatigue, à 25 et 100°C. Des essais d'usure et de fluage ont été effectués sur l'alliage et les composites non renforcés. Des examens fractographiques ont été faits pour déterminer les mécanismes de rupture en jeu.

On a découvert que même si le renforcement par des fibres améliorait les propriétés de traction et de compression aux températures élevées, les composites avaient une ductilité et une ténacité médiocres. La présence d'une couche fragile de SiO_2 aux interfaces fibres/matrice a entraîné la décohésion des interfaces en tension, nuisant beaucoup au rendement des matériaux renforcés. On a observé une certaine amélioration de la résistance à l'usure dans les matériaux composites, mais les fibres de renforcement n'ont pas amélioré sensiblement la résistance à la fatigue.

TABLE OF CONTENTS

Page

Summary i
Sommaire ii
Introduction 1
Materials 1
Chemical Composition and Density Measurements 1
Preforms 2
Microstructural Evaluation 2
Porosity and Reinforcement Distribution 2
Volume Fraction of Reinforcement 3
Microstructure of Squeeze-Cast Materials 3
Mechanical Properties Evaluation 4
Tensile Properties 4
Compression Properties 6
Impact Properties 7
Fatigue Properties 8
Wear Properties 9
Discussion 10
Conclusions 12
Acknowledgements 13
References 14

INTRODUCTION

Zinc-aluminum based alloys have found considerable industrial applications since their initial development. This is primarily due to their excellent castability, fluidity and good mechanical properties (1). Initially, Zn-Al alloys containing 35 wt % aluminum (ZA-35) were developed for their wear resistance and good bearing properties. Later, alloys with various aluminum contents, such as ZA-8, ZA-12 and ZA-27, were developed for general foundry purposes. The ZA-27 alloys are known for their high strength to density ratio and have been competing successfully against other foundry alloys such as copper, aluminum and cast iron.

Despite the attractive room temperature properties of Zn-Al alloys, their elevated temperature mechanical properties have been found to be unsatisfactory. Significant degradation of tensile strength and creep resistance occur at temperatures around 100°C. With this limitation, the extent of applications for Zn-Al alloys has been restricted to those having low temperature service environments. An attractive route towards improving the high temperature properties of Zn-Al alloys up to 150°C is by fibre reinforcement. Potential advantages include improved strength, modulus of elasticity, creep, fatigue and wear resistance. Recent work on Zn-Al has demonstrated the benefits of fibre reinforcement for these alloys (2-4). A collaborative project with the Noranda Technology Centre and the Metals Technology Laboratories (MTL) of CANMET was initiated to evaluate the microstructural, physical and mechanical properties of zinc-aluminum alloys reinforced with alumina fibres. The experimental materials were fabricated by JPL Transportation Products Inc., Engine Products Group, Cleveland, Ohio for the Noranda Technology Centre.

In this report, results on the physical (composition and density of the matrix and fibre preform), microstructural (porosity, reinforcement distribution and volume fraction, matrix microstructure) and mechanical (tensile, compression, impact, fatigue and wear) properties of these materials evaluated at CANMET and the National Research Council of Canada (NRCC) (Vancouver) are presented and discussed. The creep properties of the experimental materials were evaluated at the Noranda Technology Centre, but these results will not be presented here.

MATERIALS

CHEMICAL COMPOSITION AND DENSITY MEASUREMENTS

The materials were in the form of squeeze cast discs, with dimensions of 130 mm in diameter and 40 mm in thickness. The average chemical composition (wt %) of the squeeze cast Zn-Al alloy was evaluated as follows:

Al	Cu	Fe	Mg	Si	Zn
32.5%	2.06%	0.065%	0.012%	0.012%	balance

The composition of the squeeze-cast products complied with the standard ZA-27 foundry alloy except for the aluminum content. In performing the chemical analysis of the squeeze cast discs, a variation in composition with respect to the disc's thickness was noted. The aluminum content was higher in the upper portion of the discs whereas the Cu and Zn contents were higher in the lower portion (Fig. 1). Correspondingly, the density of the material varied as a function of the disc's thickness. This variation in composition and density is believed to be the result of the squeeze-casting parameters used to process the materials, since a similar analysis on a squeeze-cast ZA-27 disc fabricated at CANMET did not exhibit such a phenomenon. Variations in composition and density as a function of the disc's thickness were not examined in the Al_2O_3 reinforced Zn-Al composites.

Table 1 lists the values of density obtained for the three materials. Each value is the average of three or more specimens taken from the top, middle and bottom portions of the central part of a disc. Similar measurements on other discs agreed with these values within the stated standard deviations.

PREFORMS

The reinforced Zn-32Al discs were fabricated using 10 vol % and 20 vol % alumina fibre preforms made by ICI. The short Saffil alumina fibres in these preforms are reported to consist of 96-97% delta alumina and 3-4% silica (ICI product literature). This was confirmed by microprobe and powder X-ray diffraction analyses. Small portions of the preform were broken off, coated with gold and examined in the scanning electron microscope. The Al_2O_3 fibre surfaces were found to be covered by patches and films of SiO_2 (Fig. 2). The function of this SiO_2 binder is to bond the fibres together to form an interconnecting three-dimensional network. Powder X-ray diffraction analysis of crushed preform material showed the SiO_2 binder to be amorphous. The density of the preform material was 3.42 ± 0.03 g/cm^3.

MICROSTRUCTURAL EVALUATION

POROSITY AND REINFORCEMENT DISTRIBUTION

X-ray radiography was performed on the squeeze-cast discs, and the results showed that all of the discs examined were metallurgically sound.

Discs from each material (unreinforced Zn-32Al, 10 vol % Al_2O_3/Zn-32Al and 20 vol % Al_2O_3/Zn-32Al) were sectioned and polished. Specimens were examined with both

optical and scanning electron microscopes. The examination indicated that good wetting was achieved between the reinforcing alumina fibres and the zinc-aluminum matrix. There was no apparent porosity however, a few pores (about 100 μm in diameter) were observed on some of the fracture surfaces.

The fibres in the preform were aligned randomly in the transverse plane. This fibre arrangement was retained after the squeeze casting operation as shown in Fig. 3. In examining polished sections of the composites in the SEM, dark regions were revealed between fibres and at the fibre/matrix interfaces (Fig. 4). These were identified as the silicon-rich binder by energy dispersive X-ray analysis.

VOLUME FRACTION OF REINFORCEMENT

The volume fr. tions of fibres in the squeeze-cast discs were determined by quantitative metallography using a Quantimet 920 image analyser. For each of the three materials, specimens were taken from the top, middle and bottom portions of the central part of the disc and examined in the radial direction. Two hundred fields (0.8 mm^2 each) were analysed in an area of 160 mm^2 on each specimen, to quantify the fibre volume fractions. The analysis on the squeeze-cast discs indicated the volume fractions to be 12 ± 1 vol % and 24 ± 1 vol % respectively, although preforms with 10 vol % and 20 vol % Al_2O_3 were used. It is possible that the volume of the preforms was reduced during the squeeze casting operation, thereby increasing the volume fraction of fibre in the composites. Specimens of the 12 vol % Al_2O_3 reinforced Zn-32Al were evaluated using the techniques described in ASTM standard D3553 for "Fiber Content by Digestion of Reinforced Metal Matrix Composites". A volume fraction of 12.1 ± 0.4% fibre was measured, which confirmed the image analysis results.

MICROSTRUCTURE OF THE SQUEEZE-CAST MATERIALS

The binary Zn-Al phase diagram is shown in Fig. 5. The microstructure of Zn-Al alloys has been studied in detail (5,6). In the case of a sand-cast Zn-Al alloy containing 32 wt % aluminum (Zn-32Al), solidification of the melt begins with the formation of aluminum-rich dendrite cores (α phase) and then proceeds with the precipitation of proeutectic β phase around the primary dendrites. The residual liquid solidifies in the interdendritic regions according to the eutectic transformation $L \rightarrow \beta + \eta$. Upon subsequent cooling, the β phase regions transform according to the eutectoid reaction ($\beta \rightarrow \alpha + \eta$) into lamellae of α and η phases. A copper-rich ε phase ($CuZn_4$) is formed in the Zn-rich interdendritic regions in copper containing alloys. In Zn-Al alloys, iron is present in the form of faceted $FeAl_3$ inclusions.

The microstructure of the squeeze-cast Zn-32Al alloy was observed using the back scattered electron mode of the scanning electron microscope to provide an atomic contrast image (Fig. 6a). In this figure, the dark regions (1) represent the primary dendrite cores of Al-rich $\alpha + \eta$

eutectoid which are surrounded by lighter regions (2) of Zn-rich $\alpha + \eta$ eutectoid. The light regions display a continuous rim of fine η precipitates in an α matrix (3), resulting from eutectoid transformation of the proeutectic β. The white interdendritic regions (4) are Zn-rich η phase interspersed with small islands of $\alpha + \eta$ phases (5) resulting from eutectoid transformation of the eutectic β. Etching the specimen with 2% Nital revealed the presence of ε phase precipitates (6) contiguous to the interdendritic η regions (Fig. 6b).

The incorporation of fibres in the Zn-32Al alloy had a significant effect on the size of dendrites in the matrix material. As shown in Fig. 7a-c, the dendrite size is reduced as the volume fraction of fibres is increased. A higher magnification view of the fibre-reinforced Zn-32Al material shows that the dendrites have grown predominantly into the spaces between the fibres, so that the latter are surrounded by zinc-rich regions (Fig. 8a and 9a). In the 24 vol % Al_2O_3 reinforced material, the smaller spaces between the interconnecting fibres of the 20 vol % preform resulted in the smallest dendrite size. These observations eliminate the possibility of fibres acting as nucleation sites for the Al-rich primary dendrites in the matrix alloy.

In comparing the unreinforced and reinforced materials, it was also found that the volume fraction of interdendritic phases decreased with an increase in fibre volume fraction. For instance, when the volume fraction of fibres was 12%, many fibres were directly adjacent to the interdendritic η and ε phases (Fig. 8b). However, in the case of the 24 vol % Al_2O_3 reinforced composite, the percentage of η and ε phases appeared to be much smaller and most of the fibres were surrounded by Zn-rich eutectoid phases (Fig. 9a), with some ε phase regions adjacent to the fibres (Fig. 9b). A possible explanation for these observations is the effect of a lower cooling rate during the squeeze casting of the reinforced materials compared with the unreinforced alloy, due to the slower rate of heat transfer of the preheated ceramic preforms. A lower cooling rate would result in less interdendritic segregation and in a more homogeneous microstructure.

MECHANICAL PROPERTIES EVALUATION

TENSILE PROPERTIES

For tensile testing, sub-sized specimens proportional to ASTM standard E-8, with 6.35 mm gauge diameter, 25.4 mm gauge length and threaded ends were machined from the squeeze-cast discs. Testing was performed on an MTS model 810 tensile testing machine using a strain rate of 3.33×10^{-4} s^{-1} and an extensometer for recording the strain. Test temperatures were controlled within ± 1°C.

Table 2 lists the tensile test results of the squeeze-cast Zn-32Al alloy and composites. It is clear that, at room temperature, the unreinforced alloy exhibited significantly higher tensile strength than its reinforced counterparts. However, at elevated temperature, the benefits of fibre reinforcement begin to show by providing improved strength, especially in the 24 vol % Al_2O_3-

reinforced material. This is most apparent when the UTS of the unreinforced and reinforced materials are compared for the three test temperatures (Fig. 10).

The tensile elongation of the fibre-reinforced composites was also reduced in comparison with the unreinforced Zn-32Al alloy (Table 2). At room temperature, elongation values of 7 to 13% were measured for the unreinforced specimens whereas the composites showed elongations of 0.03 to 0.25%. It was therefore not possible to measure a tensile yield strength (0.2% offset) for the composites at room temperature. At elevated temperature, comparison of yield strength values at the three materials reveals similar trends to the UTS.

Fracture surfaces of unreinforced- and fibre-reinforced Zn-32Al tensile specimens were examined in the SEM. Figure 11a shows the fracture surface of a squeeze-cast Zn-32Al tensile specimen which was tested at 25°C. The surface shows quasi-cleavage interspersed with fine dimples. In some areas, fracture of $FeAl_3$ particles is evident. When this material was tested at 150°C, failure appeared to be more ductile, with larger dimples and no cleavage being present on the fracture surface (Fig. 11b). Metallographic examinations were performed on Zn-32Al tensile specimens sectioned at a plane perpendicular to the fracture surface and polished. It was noted that for specimens tested at 25°C, the fracture mode was primarily transgranular, although occasionnally cracks propagated through the η phase and along the η/zinc-rich eutectoid interfaces. When the material was tested at 150°C, the fracture path was found to proceed preferentially along the η/zinc-rich eutectoid interfaces and through the η phase, resulting in a fully interdendritic failure (Fig. 12). It is believed that, at the higher test temperatures, the transition from a transgranular to an intergranular mode of failure resulted in decreased strength and lowered ductility of the unreinforced material. This transition is likely due to the weakening of the η phase and η/zinc-rich eutectoid interfaces at elevated temperatures. These findings correlate well with the tensile strength and elongation values listed in Table 2.

In the case of the composite materials, the fracture behaviour of specimens reinforced with 12 vol % and 24 vol % Al_2O_3 fibres was found to be quite similar (Fig. 13a and 13b). Cracking proceeded preferentially along the fibre/matrix interfaces, and occasionnally along the η/zinc-rich eutectoid interfaces (Fig. 14). This suggests that the fibre/matrix interfacial strength is weaker than the η/zinc-rich eutectoid interfacial strength. In addition to fibre/matrix debonding, the fracture of fibres as well as fibre pull out were also observed on the fracture surfaces of the composites (Fig. 13a and 13b). Fine dimples were found in the matrix between the decohered and fractured fibres, but no large scale ductility was observed, even at elevated test temperatures. The fracture surfaces of reinforced specimens tested at elevated temperatures were similar to those of specimens tested at room temperature. The reduced volume fraction of interdendritic η phase, especially in the 24 vol % Al_2O_3 reinforced materials, resulted in the absence of a transition from a transgranular to an intergranular mode of failure such as was observed in the unreinforced material. The same fracture mechanisms were observed at 150°C as at 25°C, resulting in improved strength

at elevated temperature. Considering the degradation in strength of the η phase at elevated temperature, it is conceivable that the fibre/matrix interfacial strength, although weak at 25°C, nevertheless becomes higher than the η/zinc-rich eutectoid strength at 150°C.

It has been mentioned above that the SiO_2 binder, which was present on the fibre surfaces of the preform, was retained even after the squeeze-casting operation. Considering that the Al_2O_3 fibres are almost completely covered by this SiO_2 film, the fibre/matrix interfaces actually consist of Al_2O_3/SiO_2/Zn-32Al layers. It is possible that fracture could propagate either along the SiO_2/Zn-32Al or the Al_2O_3/SiO_2 interfaces, or through the SiO_2 layer. Auger Electron Spectroscopy (AES) of in-situ fracture surfaces of 24 vol % Al_2O_3 reinforced Zn-32Al showed that fracture occurs through the SiO_2 binder layer present at the fibre/matrix interface. AES point analyses and compositional depth profiles demonstrated that SiO_2 was present both on the fibre surfaces and in the depressions left in the matrix by decohered fibres (7).

COMPRESSION PROPERTIES

Compression tests were conducted at 25°C and 100°C, as per ASTM standard E-9, on cylindrical specimens (13 mm in diameter by 38 mm in length) using a strain rate of 3.33×10^{-4} s^{-1} and an extensometer for measuring the strain. Only the 0.2% offset yield strength was measured and these results are summarized in Table 3.

The compressive yield strength (CYS) of the squeeze-cast Zn-32Al is significantly higher than the tensile yield strength, especially at room temperature. This is probably related to the presence of tensile residual stresses in the material resulting from the squeeze casting operation. These possibly are relieved at 100°C, resulting in a smaller difference between the tensile and compressive properties at this temperature.

The compressive yield strength of the composites has proven to be more of a combination of the properties of the metal matrix and of the ceramic reinforcement than the tensile yield strength. It is well known that ceramics are stronger in compression than in tension. CYS increases significantly as the volume fraction of fibres increases and at 100°C, the CYS of the 24 vol % Al_2O_3/Zn-32Al is about the same as that of the unreinforced Zn-32Al at 25°C.

Some of the fibre reinforced compression specimens were loaded to failure (about 5% strain) and the resulting fracture surfaces were examined in the SEM. The fracture surfaces of the specimens were composed of shear failure of the Zn-32Al matrix with some cracked fibres (Fig. 15a). Specimens were sectioned and polished at a plane perpendicular to the fracture surface. It was observed that the extent of fibre/matrix decohesion appeared to be much reduced although there was significant fibre cracking in the region directly underneath the fracture surface (Fig. 15b and 15c). The shear stresses generated by the compressive loading caused bending and realignment of the fibres perpendicularly to the plane of maximum shear stress (Fig. 15b). This realignment was accompanied by extensive cracking of the rigid fibres. As a result of this

phenomenon, the fibres appearing on the fracture surface were mostly fractured through their thickness. It is obvious from these observations that the compressive mode of loading decreases the tendency of the reinforced materials to fail prematurely at the brittle fibre/matrix interfaces, resulting in higher properties in compression than in tension.

IMPACT PROPERTIES

Charpy impact tests were performed as per ASTM Standard E-23 on full size (10 mm x 10 mm x 55 mm) unnotched specimens. Instrumented data acquisition (Dynatup) was used to provide records of the load vs time and energy vs time traces. The measured values of Charpy impact energy of the unreinforced and reinforced Zn-32Al are listed in Table 4. In the case of the unreinforced alloy, the total impact energy was found to increase with increasing test temperatures. Despite the fact that there was a decrease in the initiation energy with an increase in test temperature, the corresponding increase in propagation energy resulted in an overall increase in impact energy. The decrease in maximum sustained load and initiation energy during impact testing at higher test temperatures is conceivable since the material starts to lose its load bearing capacity at these temperatures, as demonstrated by the tensile and compression test results. Figure 16a shows instrumented impact data for unreinforced Zn-32Al tested at 25°C. Substantial yielding occurs prior to fracture initiation as shown by the curved part of the load vs time trace before maximum load. A fair amount of energy is also spent in propagation of the crack since the load vs time trace indicates some plastic deformation occurs before the final load drop.

The fibre-reinforced composites have very poor impact toughness when compared with the unreinforced alloy (about 2.4 J compared with 85.5 J at 25°C). The effect of test temperature on the Charpy energy values of the composites was insignificant. For both the 12 vol % and 24 vol % Al_2O_3 reinforced Zn-32Al, the decreases in initiation energy and in maximum sustained load with an increase in test temperature were not as pronounced as in the case of the unreinforced alloy (Table 4). However, the propagation energy was so low that no increase in total Charpy energy has resulted. Such low propagation energy values indicate that the composites oppose little resistance to crack propagation and have low fracture toughness. Figures 16b and 16c show instrumented impact traces for the 12 vol % and 24 vol % Al_2O_3 reinforced Zn-32Al tested at 25°C. The two materials have very similar behaviour and show little evidence of yielding prior to fracture initiation. Once initiated, the crack propagates very rapidly to final fracture, requiring little energy and taking less than 0.05 ms (from the maximum load to the end of fracture) for the reinforced materials compared to about 1 m for the unreinforced alloy (Fig. 16a).

Fractographic examinations were carried out on the broken Charpy test pieces. The fracture surfaces of unreinforced Zn-32Al Charpy specimens were composed of small dimples and quasi-cleavage, with some interdendritic failure and a large number of cracked $FeAl_3$ particles. With dynamic loading (such as in impact tests) the failure modes observed in both the unreinforced

and fibre reinforced materials did not appear to change as a function of the test temperature. The fractographic features of Charpy specimens of the composite materials were very similar to those of the tensile specimens: fibre/matrix decohesion, fibre cracking and pull out, and fine dimples in the matrix. Some large porosities (about 100 μm in diameter) were observed on a few of the reinforced specimens (Fig. 17a) as well as large, cracked Al_2O_3 particles or "shot" (Fig. 17b). However these features did not appear to have had any significant effect on the fracture mode or properties. As in the case of the tensile specimens, the fractographic features of the 12 vol % and 24 vol % Al_2O_3 reinforced materials were very similar and showed very limited ductility (no shear lip formation).

FATIGUE PROPERTIES

Rotating beam fatigue tests were performed on the unreinforced and fibre reinforced Zn-32Al materials using an R.R. Moore fatigue testing machine modified to allow for elevated temperature testing (8). Standard cylindrical fatigue specimens (65 mm in length, 7.62 mm in diameter with 12.19 mm diameter tapered ends) were machined from the squeeze cast discs. The test temperature was controlled to ±1°C and the machine was run at 10 000 rpm.

Figure 18 shows a plot of stress vs cycles to failure for the three squeeze cast materials tested at 25 and 100°C. No significant effects of test temperature were observed for the Zn-32Al alloy or composites within the test result variability. In comparing the fatigue data of Al_2O_3 reinforced Zn-32Al and unreinforced Zn-32Al, the fatigue performance of the composites was found to be inferior at both the low and intermediate fatigue cycle regimes. On the other hand, the fatigue behaviour of all three materials was comparable at the high fatigue cycle regime. This would seem to indicate that at the high cycle regime, the fatigue resistance of the fibre reinforced Zn-32Al is controlled by the properties of the matrix and these are not affected by an increase in temperature from 25 to 100°C. In view of the fact that fibre reinforcement of Zn-32Al resulted in significant degradation of the tensile ductility and toughness of the alloy, it is a positive observation that no such deterioration in fatigue resistance was noted.

The fracture surfaces of selected specimens were examined in the SEM. It was found that the fractographic features of Zn-32Al specimens tested at 25°C and at 100°C were very similar. Figure 19a shows a micrograph taken from the region of fatigue crack propagation of a Zn-32Al specimen tested at 100°C. The fracture surface is very flat, with some cracked $FeAl_3$ particles visible. The region of tensile overload of the specimen had greater relief and showed similar features as on the tensile specimens (quasi-cleavage interspersed with dimples). On the 12 vol % Al_2O_3 reinforced Zn-32Al specimens, the region of fatigue crack propagation was well defined. The fatigue crack seemed to proceed mostly through the matrix, resulting in a fracture surface nearly devoid of decohered fibres and very similar to that of the unreinforced material (Fig. 19b). The region of tensile overload was similar to a tensile fracture (Fig. 19c), and as mentioned

previously, the fracture mode was dominated by fibre/matrix debonding. In the case of the 24 vol % Al_2O_3 reinforced Zn-32Al material, it was difficult to distinguish a region of fatigue crack propagation macroscopically, although small areas near the circumference of the specimen appeared to have somewhat less fibre/matrix debonding than the center regions (Fig. 19d). For all three materials, fatigue crack initiation seemed to have taken place at some defect on the specimen surface.

WEAR PROPERTIES

To characterize the wear properties of the squeeze cast Zn-32Al and composites, block on ring wear tests were carried out according to the method described by Risdon et al. (9). This test provides a rapid, first-order comparative evaluation of materials in terms of wear rate. Figure 20 shows a schematic of the block on ring equipment. Test conditions were controlled to duplicate as closely as possible the conditions used by Risdon et al. so that the data could be compared to theirs in a meaningful manner.

The test block was held rigidly against a rotating steel ring (AISI 1144) with an applied stress of 6.9 MPa. Tests were conducted at a sliding speed of 0.15 m/s with a test duration of 22 h. Most Zn-Al alloys currently in use for wear applications are subjected to similar high load (up to 6.9 MPa), low speed (0-0.3 m/s) conditions (9). The contact face of the block was ground to match closely the radius of curvature of the ring. The lubricant used for the tests was ISO grade 68 hydraulic oil, heated at 50°C. Two or three blocks were tested for each material.

Table 5 summarizes the wear test results for the squeeze cast Zn-32Al and composites and Table 6 compares these results with those of Risdon et al. for ZA-27 alloys. It was observed that the wear rate (approximately 0.7 mg/h) and friction coefficient (approximately 0.03) of the squeeze-cast Zn-32Al were both somewhat greater than those of sand-cast ZA-27, but less than the values reported for pressure die cast or permanent molded ZA-27. With the addition of 12 vol % or 24 vol % Al_2O_3 fibres, the block wear rate was rendered unmeasurable by weight loss as there was a slight net weight gain. Ring wear was also reduced. The temperature of the block and the friction force were continuously measured during the tests, and it was observed that the unreinforced Zn-32Al had a longer run-in time (time to achieve steady-state conditions) than the fibre-reinforced materials.

Although these results do indicate an improved wear resistance of the fibre-reinforced Zn-32Al compared with the squeeze-cast Zn-32Al and ZA-27 formed by various processes, more replicate results will be needed to get a better appreciation of the test result variability. The wear performance of Al_2O_3 fibre reinforced Zn-Al alloys should also be verified by field application as the actual service conditions greatly influence this property.

DISCUSSION

The present study shows that the incorporation of alumina fibres in the Zn-32Al alloy affects both the microstructure and the mechanical properties of the unreinforced alloy.

X-ray and metallographic examinations showed that the squeeze cast Zn-32Al and its Al_2O_3 reinforced composites were metallurgically sound and contained no porosities. However, chemical analysis of the squeeze cast unreinforced Zn-32Al revealed the presence of a composition gradient along the disc thickness. The upper part of the squeeze cast disc had higher aluminum content whereas the lower portion was richer in zinc and copper. Composition gradients have been observed from the top to the bottom of Zn-27Al sand castings (10). Essentially, these gradients are caused by the density difference of the different elements in the alloy. The density of pure Al is 2.71 g/cm^3 whereas the density of pure Zn is 7.14 g/cm^3. When the casting solidifies, the first solid phase to form is aluminum rich and rises to the top of the casting because of its low density compared to the melt. The zinc-rich liquid is displaced to the bottom of the casting. Such gravity segregation can be expected in sand castings because of the relatively slow cooling rates. It has been shown that this can be avoided if a sufficiently high cooling rate is used, such as in permanent mold castings (11). In the case of squeeze casting, metal molds or dies are also used. MTL's preliminary work on squeeze casting of Zn-Al alloys shows that the die should be preheated to about 350°C, and the preform should be preheated to 400°C for successful operation. The observation of gravity segregation in the squeeze-cast Zn-32Al indicates that a slow cooling rate existed because of either high die temperature or high pouring temperature.

In the Al_2O_3/Zn-32Al composite materials, it was found that, as the volume fraction of fibre reinforcement was increased, the dendrite size and volume fraction of interdendritic phases were both decreased. In a preform, the Al_2O_3 fibres are held together in a three dimensional, interconnecting network by a SiO_2 binder. During the squeeze-casting operation, the molten Zn-32Al alloy has to infiltrate this network and solidifies between the fibres. When the fibre volume fraction is increased, the fibre spacing decreases, resulting in finer dendrite sizes in the squeeze cast product. Considering that the thermal conductivity of the ceramic fibres is smaller than that of the Zn-Al alloy and that the preform is preheated prior to squeeze casting, the overall cooling rate was therefore probably lower for the reinforced castings than for the unreinforced alloy. As a result, it is expected that the extent of dendritic segregation in the reinforced alloys was lower and a more homogeneous microstructure was obtained.

From the limited test data, it was shown that fibre reinforcement improves the tensile and compression properties of Zn-32Al at elevated temperature but the improvements are accompanied by a substantial decrease in ductility and toughness. The ultimate tensile strength of the unreinforced squeeze cast Zn-32Al decreased from 404 MPa at 25°C to 156 MPa at 150°C whereas the UTS of the 24 vol % Al_2O_3 reinforced Zn-32Al decreased from 293 MPa at 25°C to

183 MPa at 150°C. The low room temperature strength and ductility of the composites were found to be caused by the presence of the brittle SiO_2 binder at the fibre/matrix interfaces. As a result, the dominant failure mode in the composite materials was fibre/matrix decohesion. In the case of the unreinforced Zn-32Al, the failure mode was transgranular at 25°C and intergranular at 150°C. This transition in the fracture behaviour is due to weakening of the interdendritic η and η/zinc rich eutectoid interfaces elevated temperatures. There was no change in the failure mode of the composites as the test temperature was raised from 25 to 150°C. This is due to the insensitivity of the fibre/matrix interfacial strength to temperature. The 24 vol % Al_2O_3/Zn-32Al composite has higher UTS than the 12 vol % Al_2O_3/Zn-32Al at 150°C (183 MPa vs 142 MPa) because of the smaller volume fraction of interdendritic phases in the composite with the higher fibre content. These results indicate that the fibre/matrix interfacial strength, albeit low at 25°C, becomes higher than that of the interdendritic η phase and η/zinc rich eutectoid interfaces at elevated temperature (12).

When the squeeze-cast materials were loaded in compression, it was found that the compressive yield strength of the 12 vol % and 24 vol % Al_2O_3 reinforced materials was higher than that of the unreinforced alloy both at room and elevated temperatures. Specimens loaded to failure revealed that, under compressive loading, the composite materials tended to fracture by ductile failure of the Zn-32Al matrix along a plane of maximum shear stress. Little fibre/matrix debonding was observed since the stresses acting upon the fibre/matrix interfaces under this mode of loading were not oriented in such a manner as to promote failure of the brittle interfacial layer.

The detrimental effect of the brittle SiO_2 layer was most pronounced when the composite materials were subjected to dynamic loading. Room temperature impact toughness of both 12 vol % and 24 vol % Al_2O_3 reinforced Zn-32Al was very low (2-3 J) and the energy values were not improved when the tests were conducted at higher temperature. As expected, the dominant failure mode under impact loading was by fibre/matrix decohesion, with a limited amount of dimpling in the matrix regions between the fibres.

The presence of the brittle SiO_2 layer at the fibre/matrix interface did not, however, appear to have a detrimental effect on the fatigue resistance of the Al_2O_3 reinforced Zn-32Al. Fractographic examinations showed that the fatigue crack path in 12 vol % Al_2O_3 reinforced Zn-32Al was mainly through the matrix, resulting in a fracture surface very similar to that of the unreinforced alloy. In comparing the fatigue data of the unreinforced and Al_2O_3 reinforced Zn-32Al, the fatigue performance of the composites was found to be inferior at both the low and intermediate fatigue cycle regimes. On the other hand, at the high cycle fatigue regime, a comparable fatigue behaviour was noted for all three materials. There have been a number of suggestions made to explain the causes of the inferior fatigue performance of composites in the low cycle regime compared to their unreinforced counterparts (13,14). In this regime, high external stresses are normally applied and the fatigue life is dominated by the rate of crack propagation.

Since metal matrix composites generally have low tensile ductility, an inferior fatigue performance is expected (13). In an investigation on an Al_2O_3/Al system (14), it was found that the presence of alumina promoted a higher fatigue crack growth rate in the composite than in the unreinforced alloy. In the case of high fatigue life regime, a low external stress is applied, and the fatigue life is more dominated by the rate of crack initiation. Premature fatigue initiation may be facilitated by fibres acting as stress concentration sites or by decohesion at the fibre/matrix interface, however no such observations were made in our examination of the Al_2O_3/Zn-32Al composites. It is possible that the improved modulus of the composites would compensate for any mechanisms which might cause degradation of the composite fatigue behaviour, thus offering a comparable fatigue performance to that of the unreinforced Zn-32Al.

It is expected that if the fibre/matrix interfacial strength could be increased, improved room temperature tensile strength, ductility and toughness could be achieved in the Al_2O_3/Zn-32Al composites. This study has demonstrated that, even under conditions of poor fibre/matrix bonding, Al_2O_3 fibre reinforcement does result in improved compression, wear and elevated temperature tensile properties without deterioration of the fatigue resistance. Fiber/matrix interfacial strength in these composites can be improved by optimizing the amount of SiO_2 binder used to hold the fibre together, thereby reducing the size and number of brittle SiO_2 patches at fibre contact points. Another alternative would be to use a different kind of binder, having better mechanical properties than SiO_2.

CONCLUSIONS

1. Alumina fibres in squeeze cast discs of Al_2O_3 reinforced Zn-32Al were found to be aligned randomly in the transverse plane, retaining the fibre arrangement of the preform. The squeeze-cast materials were metallurgically sound, with no porosity and good fibre/matrix wetting.

2. Microstructures of Zn-32Al and Al_2O_3/Zn-32Al squeeze-cast materials were composed of Al-rich primary dendrites of $\alpha + \eta$ eutectoid, of Zn-rich $\alpha + \eta$ eutectoid and of interdendritic phases composed of η and ε ($CuZn_4$). The dendrite size and volume fraction of interdendritic phases were found to decrease as the volume fraction of Al_2O_3 fibres was increased.

3. Although the unreinforced Zn-32Al had higher tensile strength than its reinforced counterparts at room temperature, reinforcement with alumina fibres did provide improved elevated temperature (100 and 150°C) tensile properties.

4. Compressive yield strength (CYS) of the squeeze-cast Zn-32Al increased significantly as the volume fraction of fibres was increased. At 100°C, the CYS of the 24 vol % Al_2O_3/Zn-32Al was still as high as the CYS of the unreinforced Zn-32Al at 25°C.

5. Charpy impact properties of the Al_2O_3/Zn-32Al composites were significantly lower than those of the unreinforced Zn-32Al. No improvements in the Charpy energy values of the composites were measured when the tests were conducted at elevated temperatures.

6. No significant effects of fibre reinforcement or of test temperature on the fatigue resistance of the Zn-32Al alloy were observed, within the test result variability.

7. Block on ring wear test results indicated an improved wear resistance of Al_2O_3 fibre reinforced Zn-32Al compared to the squeeze cast, unreinforced Zn-32Al and to ZA-27 formed by various processes.

8. Fractographic examinations performed on broken test pieces revealed that the poor ductility and toughness of the Zn-32Al composites are related to the presence of a brittle SiO_2 layer at the fibre/matrix interfaces. This SiO_2 layer, which is the binder holding the fibres together in the preform, resulted in extensive fibre/matrix decohesion under tensile and impact loading, severely impairing the performance of the reinforced materials.

ACKNOWLEDGEMENTS

The authors would like to thank Dr. M. Shehata and Mr. B. Casault (MTL, CANMET) for performing the quantitative metallographic examination; Mr. R. Bouchard, G. Weatherall and P. Fryzuk for performing the mechanical tests (tensile, compression, impact and fatigue) and V. Moore for doing the microprobe analyses.

The wear tests were conducted at the Tribology and Mechanics Laboratory of the Division of Mechanical Engineering, National Research Council of Canada (3650 Westbrook Mall, Vancouver, B.C.) by Dr. H.M. Hawthorne.

REFERENCES

1. Magnus, B., Melus, M. and Croeg, G. La Fonderie Belge 4:1927; 1982.

2. Das, A.A. et al., Int. Symp. on Zinc-Aluminum (ZA) Casting Alloys, ed. G.P. Lewis, R.J. Barnhurst and C.A. Loong; 25-5/1:1:213; 1986.

3. Guerriero, R. Parse, J. B. and Tangerini, I. ibid; 25-5/1:1:229; 1986.

4. Dent, P.N. and Murphy, S. ibid; 25-5/1:1:127; 1986.

5. Barnhurst, R.J., Gervais, E. and Bayles, F.D. AFS Transactions 91:569; 1983.

6. Sahoo, M. et al., AFS Transactions 94:225; 1986.

7. Dignard-Bailey, L., Dionne, S. and Lo, S.H. "The fracture behaviour of squeeze-cast Al_2O_3/Zn-Al composites"; Proc. Symp. on Fundamental Relationships between Microstructure and Mechanical Properties of Metal-Matrix Composites, (TMS Fall Meeting, Oct. 1989); to be published.

8. Phillips, C.E. and Thurston, R.C.A. "A note on a rotating bending - fatigue machine for tests at 200°C", Aeronautical Research Council Technical Report, R&M No. 2674, (8592); 1951.

9. Risdon, T.J., Barnhurst, R.J. and Mihaichuk, W.M. "Comparative wear rate evaluation of zinc-aluminum (ZA) and bronze alloys through block on ring testing and field applications"; SAE Paper No. 860064; 1986.

10. Sahoo, M. and Whiting, L.V. AFS Transactions 92:861-870; 1984.

11. Sahoo, M., Whiting, L.V. and White, D.W.G. AFS Transactions 93:133-144; 1985.

12. Lo, J.S.H. et al., Int. Symp. on Processing of Ceramics and Metal Matrix Composites, ed. H. Mostaghaci, The Metallurgical Society of CIM, Proceedings 17:412; 1989.

13. Nair, S.V., Tien, J.K. and Bates, R.C. Int. Met. Rev., 30:6:275; 1985.

14. Harries, S.J. and Wilks, T.E. Composite Materials 2:2.127-2.133; 1987.

Table 1. Average density of squeeze-cast Zn-32Al alloy and composites.

Material	Density (g/cm^3)
Unreinforced Zn-32Al	4.78 ± 0.05
10 vol % Al_2O_3/Zn-32Al	4.66 ± 0.03
20 vol % Al_2O_3/Zn-32Al	4.50 ± 0.03

Table 2. Uniaxial tensile test results for squeeze-cast Zn-32Al and fibre reinforced Zn-32Al composites.

Test temperature	YS (MPa)	UTS (MPa)	El (%)
Unreinforced Zn-32Al			
25°C	333±19	404±13	7-13
100°C	199±12	268±7	16-18
150°C	101±6	156±3	7-13
12 vol % Al_2O_3 reinforced Zn-32Al			
25°C	---	288±11	0.03-0.25
100°C	194±17	219±23	0.60-1.23
150°C	124±15	142±19	2.24-2.66
24 vol% Al_2O_3 reinforced Zn-32Al			
25°C	---	293±23	0.05-0.11
100°C	251±10	260±17	0.18-0.44
150°C	170±14	183±14	0.32-0.52

Table 3. Compressive yield strength for unreinforced and fibre-reinforced Zn-32Al.

Material	Zn-32Al	12 vol% Al_2O_3/Zn-32Al	24 vol% Al_2O_3/Zn-32Al
CYS (MPa) at 25°C	378 ± 5	463 ± 3	511 ± 15
CYS (MPa) at 100°C	211 ± 25	253 ± 12	355 ± 3

Table 4. Charpy impact test results of squeeze-cast Zn-32Al alloy and composites.

Material	Test temperature (°C)	Maximum load (KN)	Initiation energy* (J)	Propagation energy** (J)	Total energy (J)
Unreinforced Zn-32Al	25	16.3 ± 0.3	56.3 ± 5.1	29 ± 6	85 ± 5
	100	14.7 ± 0.3	43.8 ± 0.7	51 ± 17	95 ± 17
	150	12.5 ± 0.3	37.1 ± 2.6	93 ± 7	130 ± 6
12 vol % Al_2O_3 Zn-32Al	25	10.2 ± 1.0	2.3 ± 0.3	0.10 ± 0.04	2.4 ± 0.3
	100	9.0 ± 1.6	2.0 ± 0.9	0.20 ± 0.10	2.2 ± 0.9
	150	8.5 ± 1.6	2.1 ± 1.0	0.20 ± 0.10	2.3 ± 1.1
24 vol % Al_2O_3 Zn-32Al	25	11.9 ± 0.8	2.6 ± 0.4	0.20 ± 0.03	2.8 ± 0.4
	100	10.9 ± 0.3	2.4 ± 0.1	0.10 ± 0.01	2.5 ± 0.1
	150	10.8 ± 0.4	2.9 ± 0.3	0.10 ± 0.02	3.0 ± 0.3

*Energy at the maximum load.

**Total energy - Energy at the maximum load.

Table 5. Wear test results for squeeze-cast unreinforced and Al_2O_3 fibre-reinforced Zn-32Al.

Specimen blocks	Block weight loss (mg)	Block wear rate (mg/h)	Ring weight loss (mg)	Ring wear rate (mg/h)	Mean coefficient of friction
Zn-32Al	15.7	0.71	1.0	0.046	0.035
	14.4	0.65	3.1	0.142	0.035
12vol% Al_2O_3	(-2.4)*	---	(-0.1)	---	0.057
Zn-32Al	(-3.0)	---	0.43	0.020	0.058
24vol% Al_2O_3	(-3.6)	---	0.1	0.005	0.057
Zn-32Al	(-3.2)	---	0.5	0.023	0.044
	(-2.2)	---	0.42	0.019	0.039

*Bracketted figures indicate weight gain.

Table 6. Comparison of wear and friction measurements for Zn-32Al and composites with data of Risdon et al. (9) for ZA-27.

Material	Wear rate (mg/h)	Friction coefficient
Sand cast ZA-27 (<0.2 vol % porosity)*	0.13	0.01
Sand cast ZA-27 (0.5-1.0 vol % porosity)*	0.24-0.36	0.01
Pressure die cast ZA-27*	1.02	0.08
Permanent molded ZA-27*	1.4-4.5	0.03-0.07
Squeeze Cast Zn-32Al	0.65-0.71	0.035
12 vol% Al_2O_3 / Zn-32Al	nil**	0.057-0.058
24 vol% Al_2O_3 / Zn-32Al	nil**	0.039-0.057

* Composition of ZA-27 (wt %): 25.0-28.0 Al, 2.0-2.5 Cu, 0.01-0.02 Mg (9).

** Weight gain of the blocks was measured.

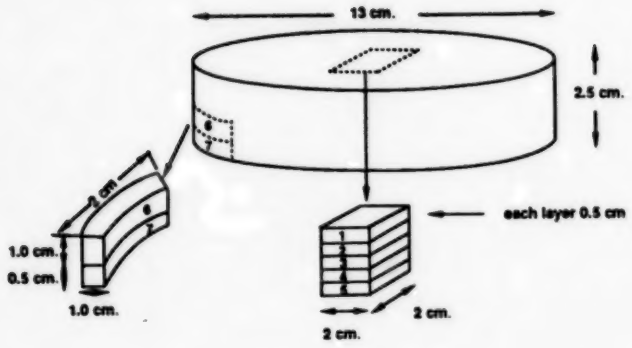

	Composition (wt %)			Density
	Al	Cu	Zn	(g/cc)
1	35.1	2.1	62.8	4.62
2	35.3	2.1	62.6	4.66
3	34.3	2.2	63.5	4.76
4	33.2	2.2	64.6	4.79
5	30.2	2.3	67.5	4.87
6	31.2	2.3	66.5	4.81
7	25.5	2.5	72.0	5.11

Fig. 1. Variation of composition and density with respect to disc's thickness in an unreinforced, squeeze-cast disc.

Fig. 2. SEM micrograph of preform.

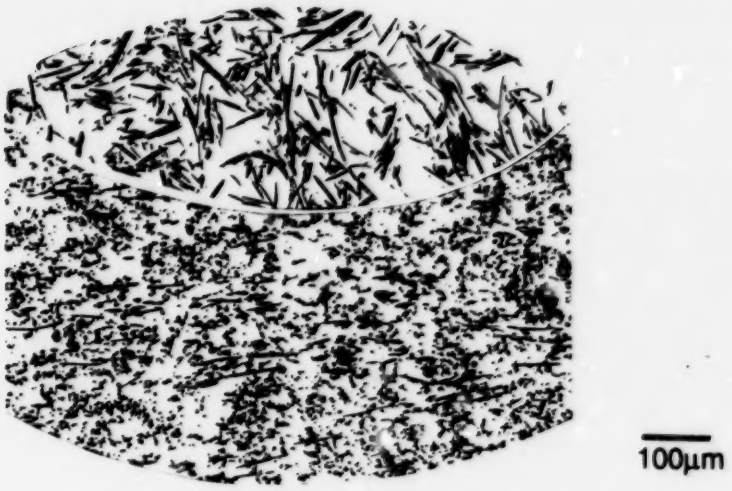

Fig. 3. Optical micrograph of as-polished 24 vol % Al_2O_3/Zn-32Al composite showing reinforcement distribution.

Fig. 4. SEM micrograph of polished section of 24 vol % Al_2O_3/Zn-32Al composite showing SiO_2 films between the fibres (arrows).

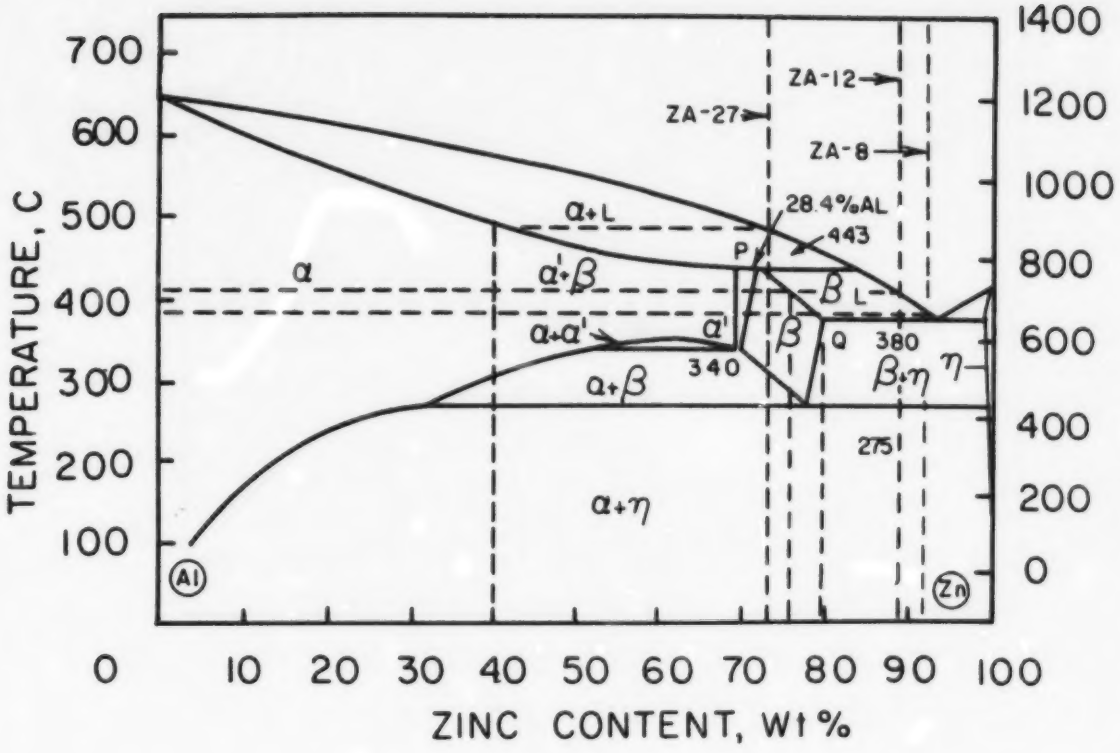

Fig. 5. Al-Zn equilibrium phase diagram.

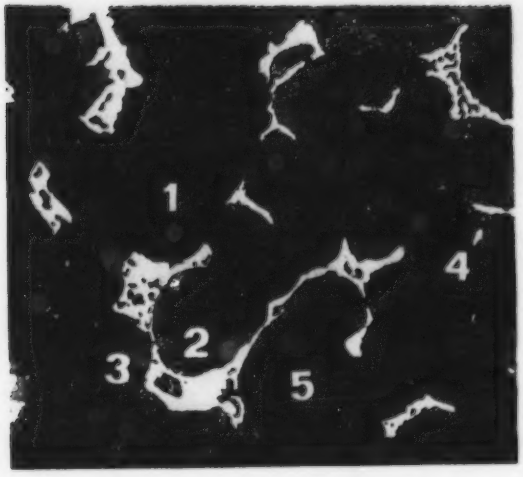

Fig. 6a. ·mic contrast micrograph (BSE) of as-polished, unreinforced squeeze-cast Zn-32Al.

Fig. 6b. SE micrograph of Nital etched, unreinforced squeeze cast Zn-32Al.

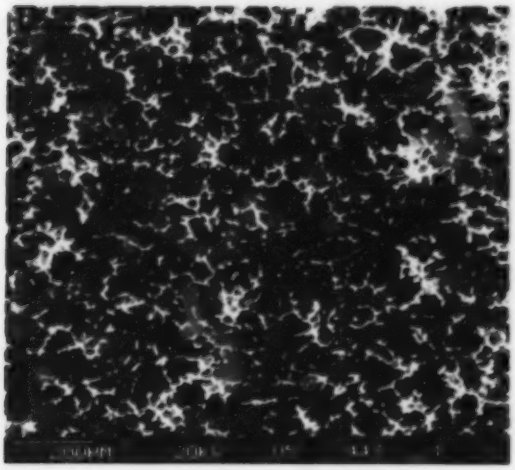

Fig. 7a. Unreinforced squeeze-cast Zn-32Al.

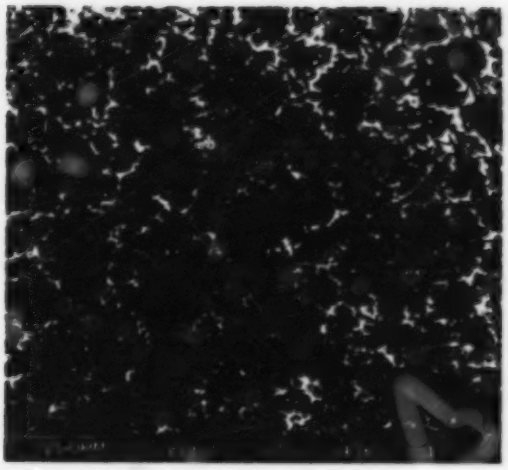

Fig. 7b. 12 vol % Al_2O_3 reinforced Zn-32Al (planar view).

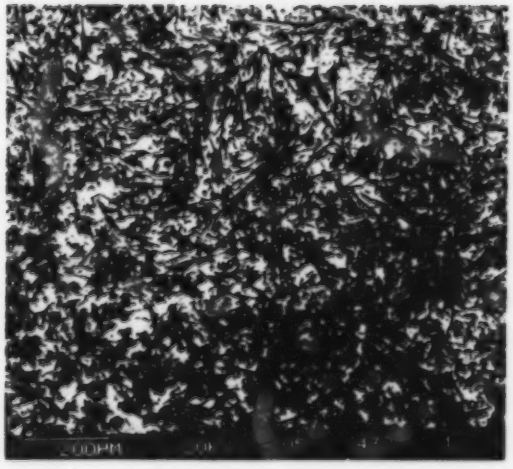

Fig. 7c. 24 vol % Al_2O_3 reinforced Zn-32Al (planar view).

Fig. 8a. Atomic contrast micrograph (BSE) of as-polished, 12 vol % Al_2O_3 reinforced Zn-32Al composite (planar view).

Fig. 8b. SE micrograph of Nital etched, 12 vol % Al_2O_3 reinforced Zn-32Al composite (planar view).

Fig. 9a. Atomic contrast micrograph (BSE) of as-polished, 24 vol % Al_2O_3 reinforced Zn-32Al composite (planar view).

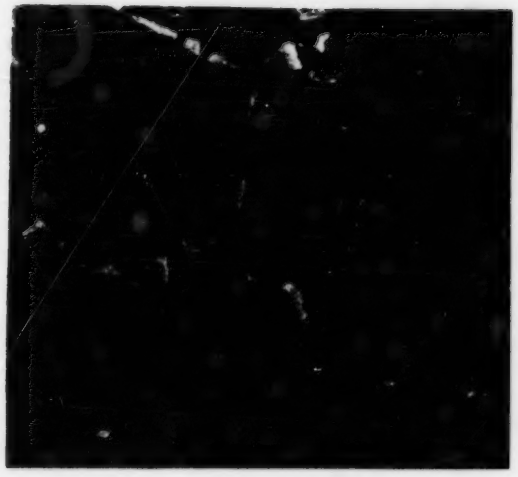

Fig. 9b. SE micrograph of Nital etched, 24 vol % Al_2O_3 reinforced Zn-32Al composite (planar view).

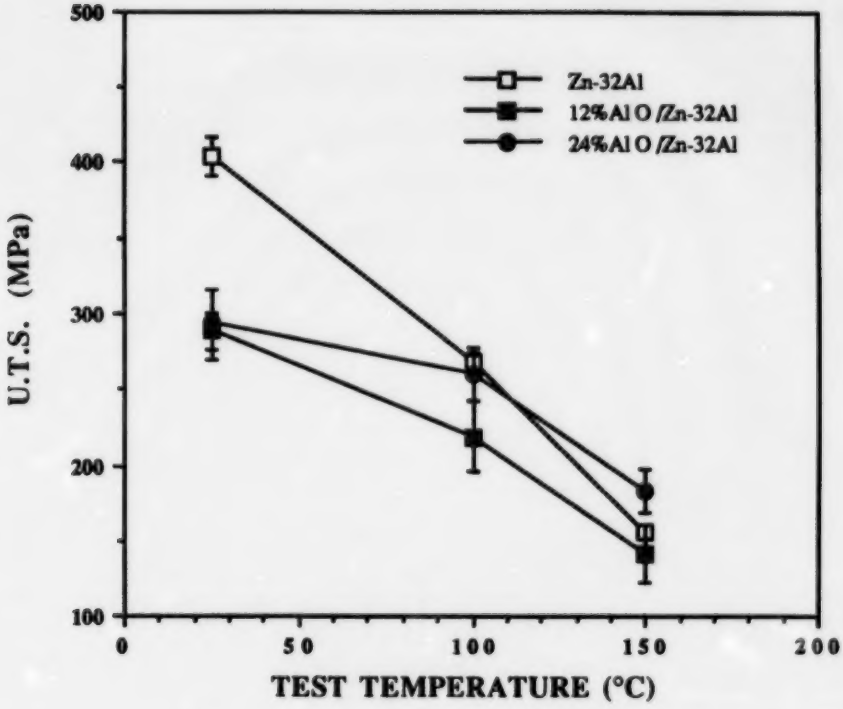

Fig. 10. Plot of UTS as a function of test temperature for squeeze-cast Zn-32Al alloy and composites.

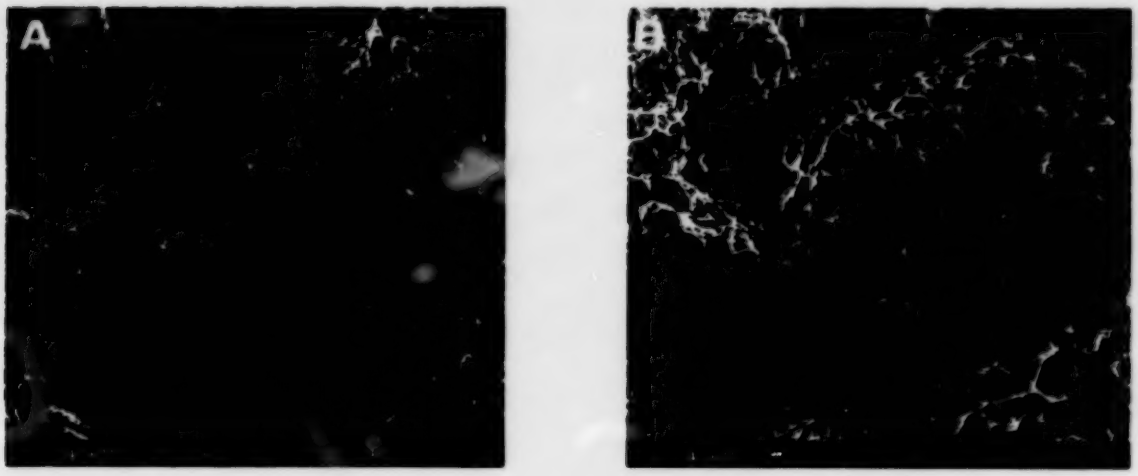

Fig. 11. SE fractograph of squeeze cast unreinforced Zn-32Al tensile specimen tested at (a) 25°C and (b) 150°C.

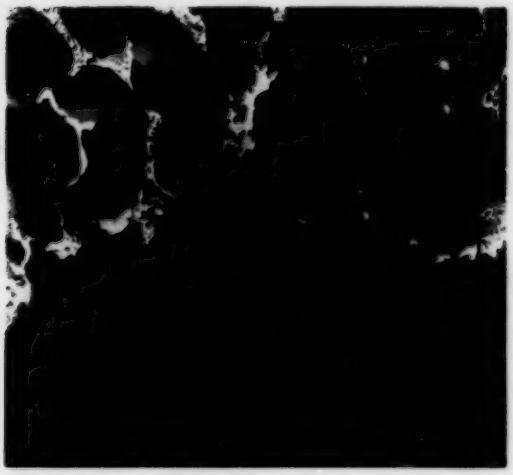

Fig. 12. Atomic contrast micrograph (BSE) of a sectioned and polished tensile specimen of squeeze-cast, unreinforced Zn-32Al tested at 150°C, showing the $\eta + \varepsilon$ interdendritic phases at the fracture surface.

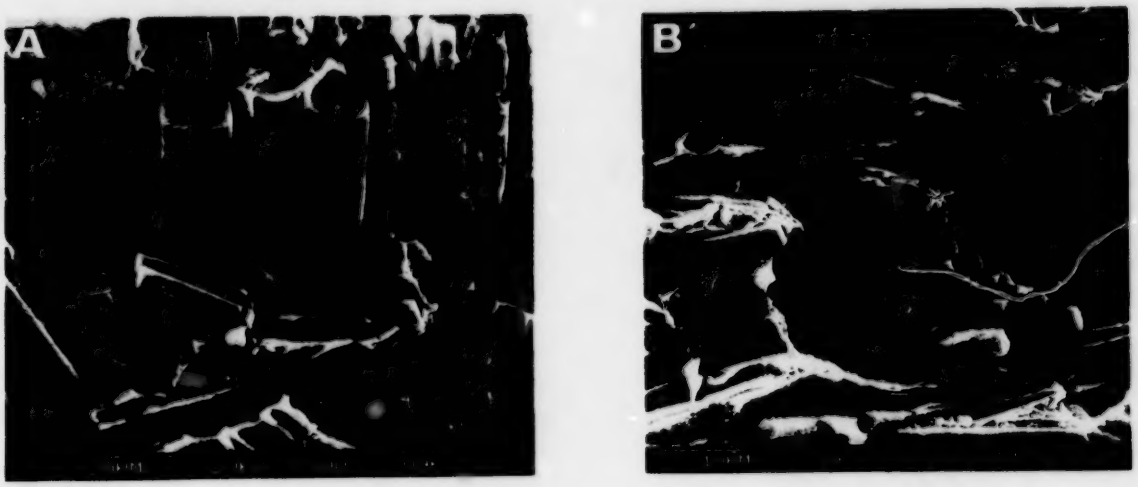

Fig. 13. SE fractographs of (a) 12 vol % Al_2O_3 reinforced and (b) 24 vol % Al_2O_3 reinforced Zn-32Al tensile specimens tested at 25°C.

Fig. 14. Atomic contrast micrograph (BSE) of a sectioned and polished tensile specimen of 24 vol % Al_2O_3 reinforced Zn-32Al tested at 25°C, showing fibre/matrix debonding and fibre cracking.

Fig. 15a. SE micrograph of fracture surface of a 24 vol % Al_2O_3 reinforced Zn-32Al specimen failed in compression at 25°C.

Fig. 15b. Polished and etched section perpendicular to the fracture surface of a 24 vol % Al_2O_3 reinforced Zn-32Al specimen failed in compression at 25°C.

Fig. 15c. Polished and etched section perpendicular to the fracture surface of a 24 vol % Al_2O_3 reinforced Zn-32Al specimen failed in compression at 25°C.

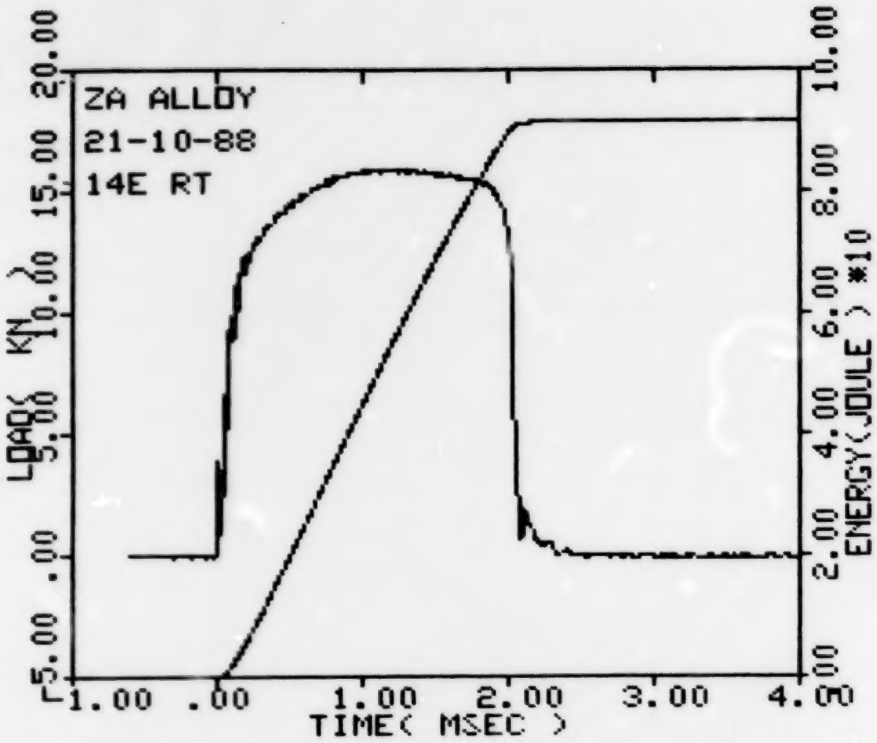

(a) unreinforced Zn-32Al

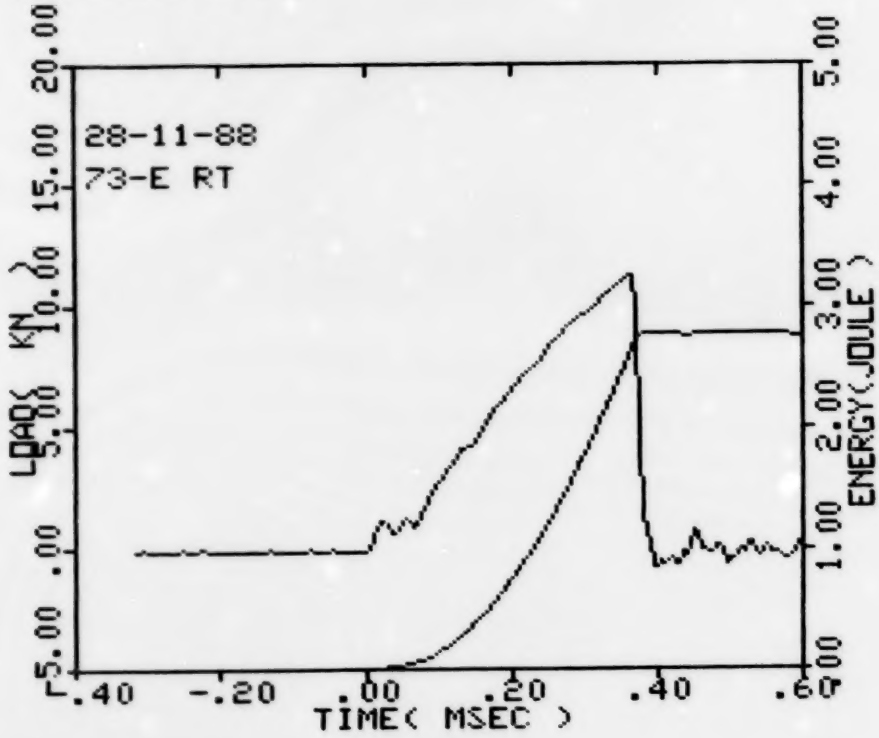

(b) 12 vol % Al_2O_3 reinforced Zn 2Al

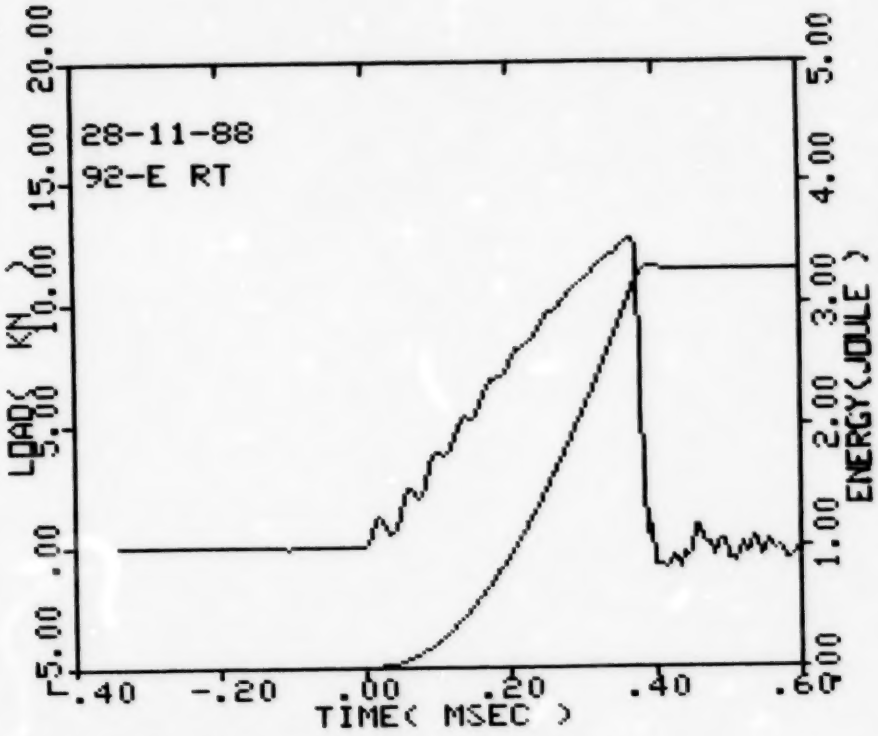

(c) 24 vol %Al_2O_3 reinforced Zn-32Al tested at 25°C.

Fig. 16. Instrumented impact traces

Fig. 17a. SE fractograph of a 24 vol % Al_2O_3 reinforced Zn-32Al Charpy specimen tested at 25°C showing a large porosity.

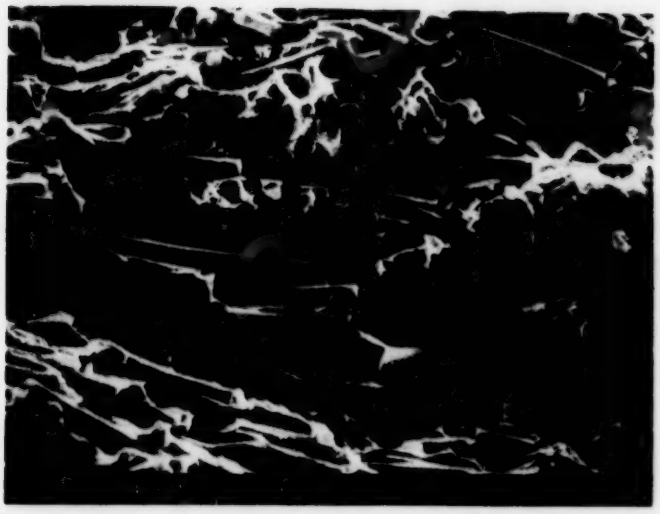

Fig. 17b. SE fractograph of a 24 vol % Al_2O_3 reinforced Zn-32Al Charpy specimen tested at 25°C showing large, cracked, irregularly shaped Al_2O_3 particle.

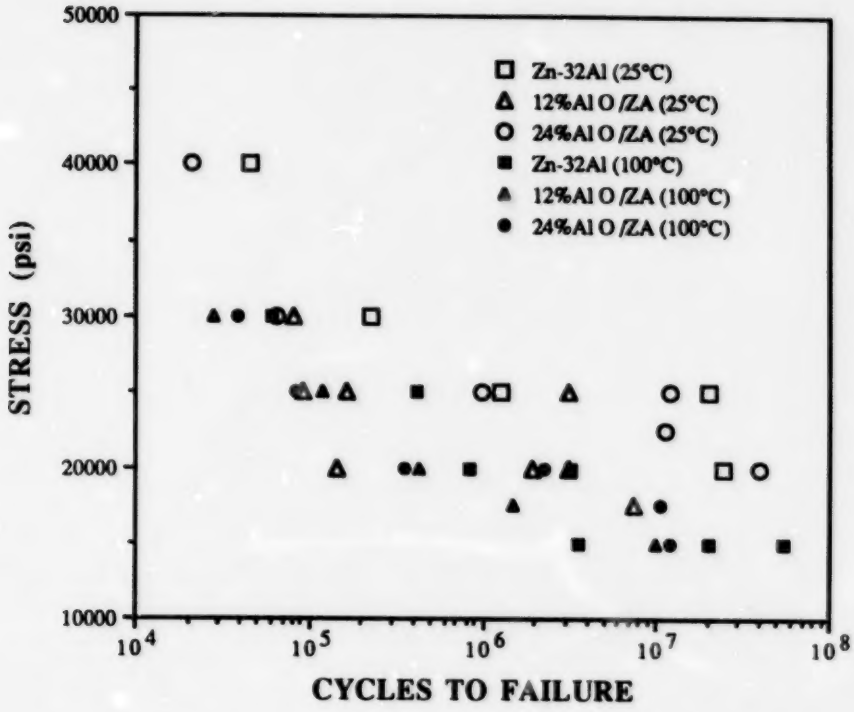

Fig. 18. Fatigue data for squeeze cast Zn-32Al alloy and composites.

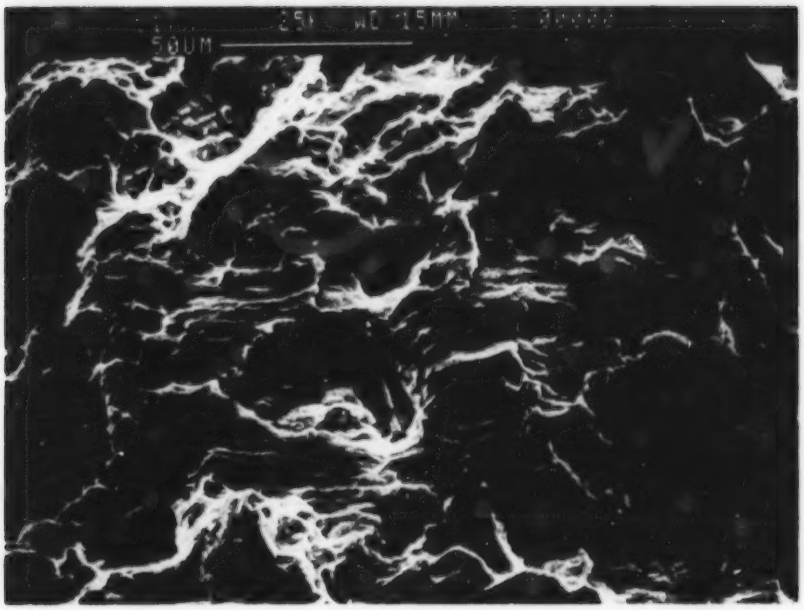

Fig. 19a. SE micrograph of a fatigue specimen of Zn-32Al tested at 100°C (region of fatigue crack propagation).

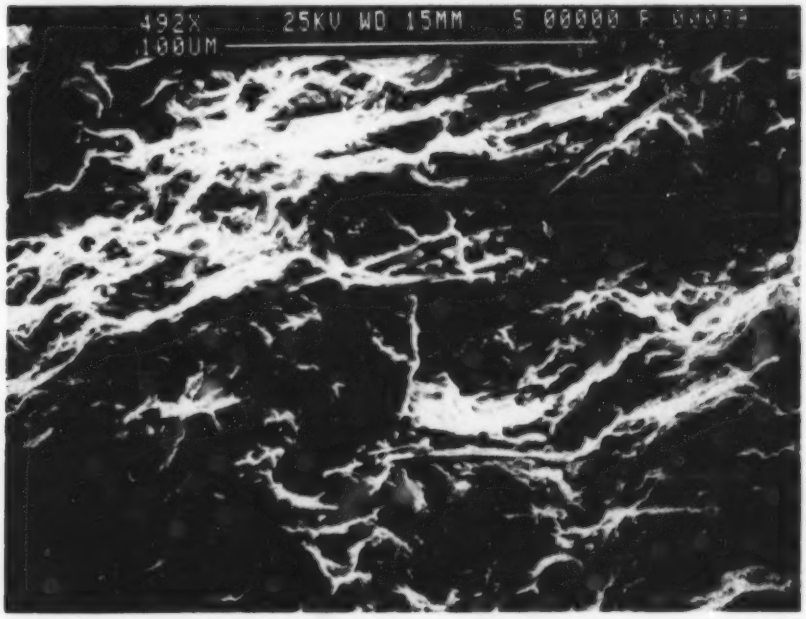

Fig. 19b. SE micrograph of a fatigue specimen of 12 vol % Al_2O_3 reinforced Zn-32Al tested at 25°C (region of fatigue crack propagation).

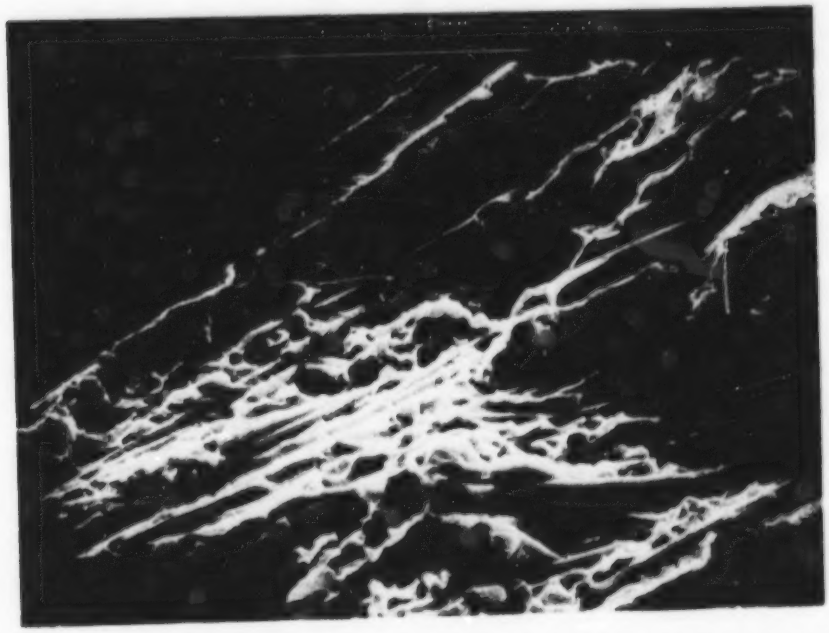

Fig. 19c. SE micrograph of a fatigue specimen of 12 vol % Al_2O_3 reinforced Zn-32Al tested at 25°C (region of tensile overload).

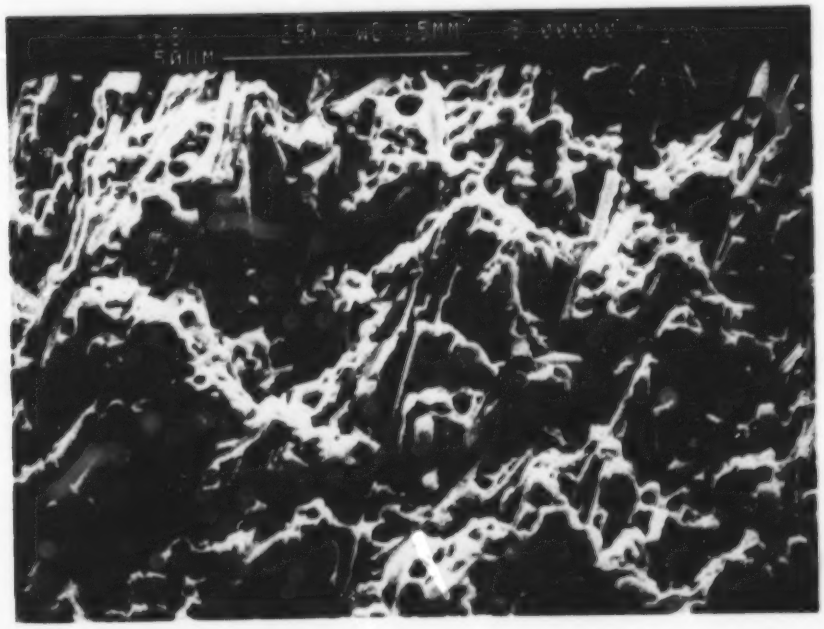

Fig. 19d. SE micrograph of a fatigue specimen of 24 vol % Al_2O_3 reinforced Zn-32Al tested at 100°C (region of fatigue crack propagation).

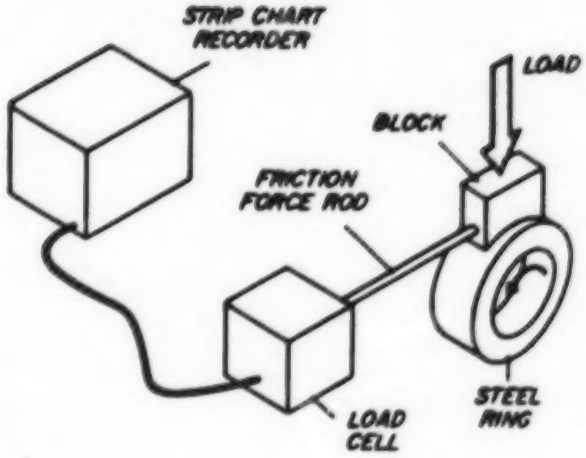

Fig. 20. Schematic of block on ring test equipment (9).

FIGURE IDENTIFICATION

Figure	Micrograph ID	Neg. No.
Fig. 13a	(096)	19729
Fig. 15a	(00059)	19730
Fig. 17a	(120)	19727
Fig. 17b	(122)	19726
Fig. 19a	(00047)	19733
Fig. 19b	(00039)	19731
Fig. 19c	(00045)	19732
Fig. 19d	(00020)	19728